Since January 2020 Elsevier has created a COVID-19 resource centre with free information in English and Mandarin on the novel coronavirus COVID-19. The COVID-19 resource centre is hosted on Elsevier Connect, the company's public news and information website.

Radiotherapy and Oncology 153 (2020) 289–295

Contents lists available at ScienceDirect

Radiotherapy and Oncology

journal homepage: www.thegreenjournal.com

Original Article

Low dose radiation therapy for COVID-19: Effective dose and estimation of cancer risk

Trinitat García-Hernández [a,*], Maite Romero-Expósito [b], Beatriz Sánchez-Nieto [c]

[a] Department of Medical Physics, ERESA, Hospital General Universitario, Valencia, Spain; [b] Área de Ciencias Básicas y Ambientales, Instituto Tecnológico de Santo Domingo (INTEC), P.O. Box 342-9/249-2, Santo Domingo, Dominican Republic; [c] Instituto de Física, Pontificia Universidad Católica de Chile, Santiago, Chile

ARTICLE INFO

Article history:
Received 2 August 2020
Received in revised form 16 September 2020
Accepted 27 September 2020
Available online 14 October 2020

Keywords:
COVID-19
Lifetime attributable risk
Effective dose
Cancer Risk
Low dose radiation therapy

ABSTRACT

Background and purpose: The objective of this work is to evaluate the risk of carcinogenesis of low dose ionizing radiation therapy (LDRT), for treatment of immune-related pneumonia following COVID-19 infection, through the estimation of effective dose and the lifetime attributable risk of cancer (LAR).

Material and methods: LDRT treatment was planned in male and female computational phantoms. Equivalent doses in organs were estimated using both treatment planning system calculations and a peripheral dose model (based on ionization chamber measurements). Skin dose was estimated using radiochromic films. Later, effective dose and LAR were calculated following radiation protection procedures.

Results: Equivalent doses to organs per unit of prescription dose range from 10 mSv/cGy to 0.0051 mSv/cGy. Effective doses range from 204 mSv to 426 mSv, for prescription doses ranging from 50 cGy to 100 cGy. Total LAR for a prescription dose of 50 cGy ranges from 1.7 to 0.29% for male and from 4.9 to 0.54% for female, for ages ranging from 20 to 80 years old.

Conclusions: The organs that mainly contribute to risk are lung and breast. Risk for out-of-field organs is low, less than 0.06 cases per 10000. Female LAR is on average 2.2 times that of a male of the same age. Effective doses are of the same order of magnitude as the higher-dose interventional radiology techniques. For a 60 year-old male, LAR is 8 times that from a cardiac CT, when prescription dose is 50 cGy.
 Radiotherapy and Oncology 153 (2020) 289–295

The ongoing pandemic of COVID-19 disease is spreading rapidly all over the world, collapsing medical systems and causing spikes of deaths in many countries. However, until now, there is no effective treatment for COVID-19 immune-mediated pneumonia.

Radiotherapy (RT) administered at low doses modulates the inflammatory response, producing an anti-inflammatory effect. During the early part of the past century low-dose ionizing radiation therapies (LDRT) were effectively used to treat pneumonia [1–4]. Some more recent articles [5,6] showed LDRT as a potential treatment for inflammatory disease. Based on this previous experience, some authors propose LDRT as an alternative treatment for immune-related pneumonia following COVID-19 infection [7–9].

Currently, there are several clinical trials underway to test the efficacy of LDRT [10–13]. The literature suggests that doses between 0.3 and 1 Gy [5] incite anti-inflammatory properties, while doses >2 Gy induce the production of proinflammatory cytokines, leading to an inflammatory response. The proposed total dose in most of the new COVID-19 radiotherapy clinical trials is below 1 Gy, in one or two fractions. This low prescription dose is at least one order of magnitude lower than typical doses of radiotherapy treatments. Thus, even for organs inside or partially inside the treatment fields (such as heart, oesophagus, etc..), doses are well below the limiting doses for normal tissues and deterministic effects (i.e., harmful tissue reactions) are not expected. However, epidemiological and experimental studies provide evidence of the probability of incurring cancer at doses about 100 mSv or less [14]. Although it is not clear whether cancer risk has a threshold or not, in radiation protection the linear no-threshold (LNT) model of cancer risk is accepted, which implies that there is no safe dose of ionizing radiation [15]. For the low dose levels in LDRT, stochastic risks are expected to be small, but they must be quantified. Even if clinical trials show a good performance of LDRT for treating COVID-19 pneumonia, cancer risk estimation is required in order to evaluate the risk–benefit balance of the treatment. Therefore, the objective of this work was to assess the risk of carcinogenesis after LDRT for COVID-19 pneumonia by the estimation of effective dose and the Lifetime Attributable Risk (LAR) of cancer.

* Corresponding author at: Department of Radiation Oncology, ERESA, Hospital General Universitario, Avda. Tres Cruces, 2, Valencia E-46014, Spain.
E-mail address: mtrinitat.movil@gmail.com (T. García-Hernández).

https://doi.org/10.1016/j.radonc.2020.09.051
0167-8140/

Material and methods

Planning

COVID-19 RT plans were designed, for a Varian Truebeam linear accelerator, in the Pinnacle radiotherapy Treatment Planning System (TPS) version 16.0.2 (©Koninklijke Philips), on the adult Reference Male and Reference Female computational phantoms from the International Commission on Radiological Protection (ICRP) [16]. Both phantoms permitted the identification of organs and tissues explicitly noted in the definition of effective dose. The planning target volume (PTV) included both lungs plus a margin of 0.5 cm in all directions.

The treatment plan evaluated was a 3D Conformal Radiotherapy Technique (3DCRT) with anterior and posterior 6 MV fields, weighted to minimize hot spots. The collimators were rotated to 90 degrees to optimize normal tissue shielding (see Fig. 1). At least 95% of PTV receives 95% of the prescribed dose. No additional dose restrictions were imposed on any organ at risk. Based on current clinical trials [10–13] three prescription doses were used: 50 cGy and 70 cGy in one fraction, and 100 cGy in two fractions.

Dosimetry

Effective dose and cancer risk rely on an initial comprehensive evaluation of equivalent dose in organs. In this work, tissues and organs investigated are listed in Table 1.

Given that treatments only imply exposure to photons, equivalent dose equals absorbed dose, which could be extracted from TPS data. However, the accuracy of TPS outside the border of the field has been questioned [17,18]. Consequently, in this work the Dose Volume Histogram (DVH) information provided by the TPS was only used to determine the mean absorbed dose administered to organs inside the 5% isodose (i.e., approximately up to 3–4 cm of the border of the field). Outside the 5% isodose, an ad-hoc peripheral dose model was built for the LDRT plans by measuring the out-of-field dose on a geometrical phantom. Skin dose was estimated from in and out-of field measurements through EBT3 radiochromic films.

A detailed description of the procedure followed to calculate equivalent dose is available as supplementary material.

Table 1
Equivalent dose in tissue/organs and effective dose, per unit of prescription dose, for the Reference male and Reference female phantoms.

Organs and tissues	Equivalent dose per prescribed dose (mSv/cGy)	
	Male	Female
Brain	0.044	0.092
Salivary glands	0.18	0.28
Thyroid§	3.6	4.1
Oesophagus	7.3	8.1
Lung§	10	10
Stomach	4.7	4.2
Breast§	8.2	9.8
Liver	4.1	4.2
Colon	0.31	0.12
Gonads (testicles/ovaries)	0.0051	0.0078
Bladder	0.012	0.010
Bone marrow (red)	2.1	2.0
Bone Surface	2.0	1.9
Skin	1.5	1.5
Remainder tissues*	3.1	3.3
Prostate#	0.0051	
Uterus#		0.0086
Heart§ ▫	10	10
Effective dose	**4.1**	**4.3**

§ Dose obtained only from TPS.
* In this work: Adrenals, extrathoracic (ET) region, gall bladder, heart, kidneys, muscle, pancreas, prostate (♂), small intestine, spleen, thymus and uterus/cervix (♀).
# Equivalent doses additionally reported for *LAR* calculation.
▫ Dose reported just for discussion.

Effective dose calculations

The effective dose was calculated as the tissue-weighted sum of the equivalent dose in all specified tissues and organs according to ICRP report 103 [19].

Cancer risk calculations

As mentioned in the introduction, LDRT prescription dose is below 1 Gy, delivered either in one or two fractions. BEIR-VII report judged that the LNT model provided the most reasonable description of the relation between low-dose exposure to ionizing radiation and the incidence of cancers that are induced by ionizing

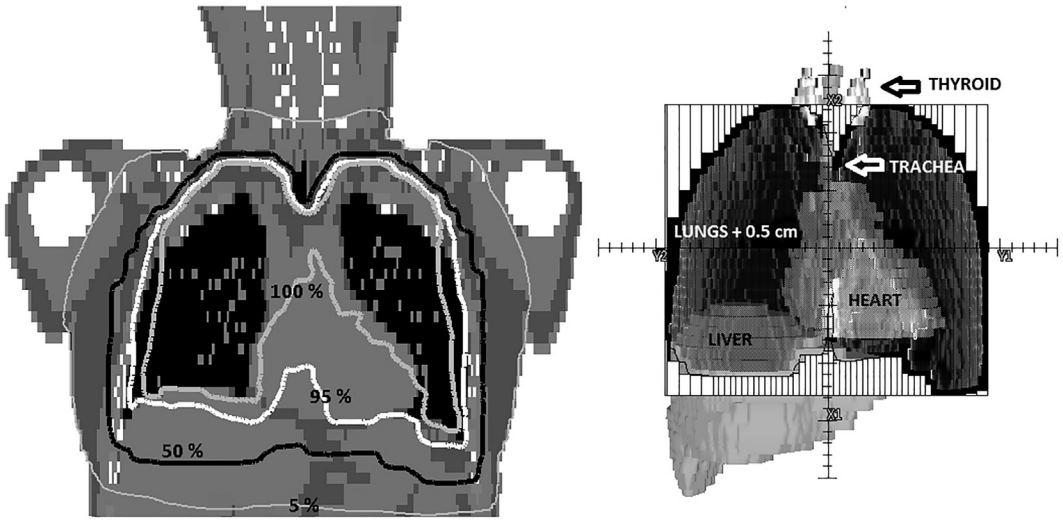

Fig. 1. On the left, dose distribution in a coronal plane with labeled relative isodose lines (normalized to the prescription dose). On the right, the beam's eye view of the anterior field. The vertical lines represent the multileaf collimator. Lungs + 0.5 cm (PTV) can be seen in dark grey together with the thyroid (light grey), trachea (grey), liver (grey), and heart (grey). Thyroid and liver are partially outside the field, depicted by the outer rectangular solid line.

radiation [20]. In the present work, the LNT model [20] was used, and cancer risk was estimated as the LAR of cancer incidence (excess risk for the rest of the life since treatment). Following the guidelines by the BEIR-VII report, LAR of cancer incidence by cancer site is calculated multiplying equivalent dose in organ by the organ-specific incidence risk coefficient. Total LAR is obtained by the addition of cancer risks associated to each organ.

Both age-at-exposure and sex are relevant parameters for carcinogenesis. Therefore, we used the sex- and age-specific coefficients from table 12D-1 in BEIR-VII report [20] to calculate LAR for several ages (20, 30, 40, 50, 60, 70, 80) for both the male and female phantoms.

Another consequence of the exposure of the patient to a low dose range is that different fractionation regimes are expected to generate a similar risk of inducing cancer [21]. However, it was decided to quantify the effect of delivering the dose in one or two fractions on the risk of inducing lung cancer (the organ receiving the highest dose). In order to do that, a more sophisticated dose–response model, which incorporates all relevant phenomena occurring during fractionated exposure, was used. In particular, the Schneider's model [22–25] was chosen. A detailed description of the use of this model can be found in Sánchez-Nieto et al. 2017 [26]. The parameters of the model were taken from Schneider et al. 2011 [24]. LAR for lung cancer was estimated for 1 Gy administered in either one or two fractions.

Results

Table 1 shows the equivalent dose in organs, per unit of prescribed cGy, employed to calculate effective dose and LAR. The highest dose is received by the lung, breasts, and oesophagus (doses in the range of the prescription dose) and the lowest, for organs far away from the field border, such us, gonads, prostate, or uterus (doses two orders of magnitude lower than the prescription dose). The differences of equivalent dose in organs between male and female are small, due mainly to structure and volume differences. Consequently, the effective dose per unit of prescribed cGy for male and female is also similar, around 4 mSv/cGy. The main contributors to effective dose are lungs, breasts and stomach (30%, 13% and 26% of effective dose on average, respectively). Total treatment leads to an effective dose for male/female of 204/213 mSv, 286/298 mSv and 408/426 mSv for prescription doses of 50 cGy, 70 cGy and 100 cGy, respectively.

Table 2 shows LAR of cancer incidence by cancer sites for a prescription dose of 50 cGy of a LDRT treatment of COVID-19 pneumonia as a function of patient age for male and female. Results can be re-escalated (multiplying by 1.4 for a total dose of 70 cGy and for 2 for a total dose of 100 cGy) to obtain LAR for the other prescription doses.

As can be noticed, the larger contribution to cancer risk for the reference male comes from lung and remainder (mainly due to the high dose in heart – see Table 1), with 80% of the total LAR. LAR calculations on the female phantom reveal lung and breast as the cancer sites with larger risk (together with remainder represent 90% of total LAR). The contribution of breast is especially relevant for young women. While for a 20 year-old woman breast LAR represents 42% of total, for a 50 year-old woman, the proportion is reduced to 18%.

Fig. 2 shows estimates of the LAR (in %) by sex corresponding to the three prescription doses as a function of age. It is worth to notice the different range of the LAR estimates for males (from 1.7% to 0.29% for 50 cGy prescription dose) and females (from 4.9% to 0.5% for 50 cGy prescription dose). The average ratio between females LAR and males LAR is 2.2, being 3.0 at 20 years and reducing up to 1.8 at 80 years. The highest LAR in females can be explained by several facts. First, breast cancer risk is only considered for the female. Also, organs receiving the highest doses, lung and breast, are organs very radiosensitive, especially for females. For example, risk coefficient of lung for female is on average 2.3 times the value for male.

The age dependence of LAR can be noticed both in Table 2 and Fig. 2. As age increases, LAR reduces. Total LAR for cancer incidence at 60 years is 2 or 3 times less than at 20 years. In this sense, although trials accept young people, it is known that severe COVID-19 mainly affects people older than 60 years old, those for whom cancer risk significantly reduces. For the highest prescription dose (total dose of 100 cGy), LAR at 60 years is 1.6% for males and 3.0% for females. For 80 year-old patients, very affected by severe COVID-19, LAR reduces to less than half of that at 60 years old (0.59% and 1.1%, respectively).

Ongoing clinical trials have different fractionation schemes, mainly consisting of one fraction. However, there is a scheme consisting of a first fraction of 50 cGy complemented, if necessary, with a second fraction of the same dose. LAR of lung cancer incidence was calculated using the Schneider model for 100 cGy administered in one or two fractions of 50 cGy. It is noteworthy that the LAR found for one fraction was lower than for two fractions for both sexes and all ages. Nevertheless, as the relative difference was below 1%, in fact both fractionation schemes can be considered very similar from the point of view of the risk of inducing lung cancer. Therefore, for the low dose range of LDRT, this indicates that fractionation has negligible effect on carcinogenesis.

Discussion

Effective dose is accepted as a useful indicator of patient exposure enabling different exposures to be compared meaningfully, taking into account the relative radiosensitivities of organs involved. However, it has to be only used as an instrument for comparison of different radiological techniques. As shown by our results, while male and female adults would receive almost the same effective dose, the impact on cancer risk is different. In fact, not only the sex of the patient is relevant, but the age also plays an important role. Thus, effective dose is not recommended for epidemiological evaluation of cancer risk, and other quantities, such as LAR, should be used.

Table 3 summarizes typical effective doses for different radiology techniques, as reported in the literature, compared to COVID-19 LDRT. Based on this data, effective dose found in our work is of the same order of magnitude than the interventional radiology techniques with the highest exposure, such as transjugular intrahepatic portosystemic shunt placement (180 mSv) and abdominal aortic endoprosthesis (166 mSv; range 61.2–380.8 mSv). Also, COVID-19 LDRT, for a prescription dose of 50 cGy, corresponds to approximately 11 and 8 thorax and abdomen scans with the highest dose protocols, 7 4DCT, 7 whole body high-quality PET/CTs, 7 cardiac CTs (retrospective EGC-gated coronary computed tomography angiography) and 5 cardiac stress-rest tests using thallium 201 chloride. If a total dose of 100 cGy is administered for COVID-19 pneumonia treatment, the number of equivalent examinations should be doubled.

Table 4 shows estimates of cancer incidence associated with some radiology procedures. For a 20 year-old woman, the highest LAR corresponds to a whole body PET/CT or cardiac CT, with a value of around 0.5%, which is approximately 10 times less than LAR for COVID-19 LDRT prescribed at 50 cGy. Also, a routine chest CT shows a LAR of cancer incidence almost 20 times less risk than COVID-19 LDRT, for a 20 year-old female. For older patients, such as a 60 year-old man, LAR for COVID-19 LDRT is 8 times that associated with a cardiac CT and 5 times that from a myocardial

Table 2
Lifetime attributable risk (cases per 10,000) of cancer incidence for a 50 cGy radiotherapy treatment of COVID-19 for male and female computational phantoms as a function of age at exposure. The range of age-at-exposure is compatible with that eligible for current COVID-19 LDRT trials (between 18 and 60 years).

Cancer site	Age at exposure (years)						
	20	30	40	50	60	70	80
Male							
Thyroid	3.8	1.6	0.55	0.18	0.055	0.018	0.0
Lung	77	54	54	52	46	34	18
Stomach	9.3	6.5	6.3	5.8	4.7	3.3	1.6
Liver	6.2	4.5	4.3	3.9	2.9	1.7	0.62
Colon	2.7	1.9	1.9	1.8	1.5	1.0	0.47
Bladder	0.059	0.043	0.043	0.042	0.036	0.026	0.013
Prostate	0.012	0.009	0.009	0.0085	0.0067	0.0036	0.0013
Leukemia	9.9	8.7	8.7	8.7	8.5	7.6	5.0
Remainder*	57	36	31	26	18	10	4.2
Female							
Thyroid	23	8.4	2.9	0.82	0.2	0.061	0.0
Lung	180	120	120	120	100	75	39
Stomach	11	7.6	7.4	6.8	5.7	4	2.3
Breast	210	120	69	34	15	5.9	2.0
Liver	3.0	2.1	2.1	1.9	1.5	1.1	0.42
Colon	0.67	0.48	0.46	0.43	0.36	0.26	0.13
Bladder	0.054	0.039	0.039	0.037	0.032	0.023	0.012
Uterus	0.011	0.0077	0.0069	0.0056	0.0039	0.0021	0.00086
Ovary	0.020	0.013	0.012	0.0098	0.0070	0.0043	0.0020
Leukemia	7.0	6.2	6.1	6.1	5.7	5.1	3.7
Remainder*	60	39	34	28	20	13	5.6

* Remainder in LAR calculations does not include prostate and uterus.

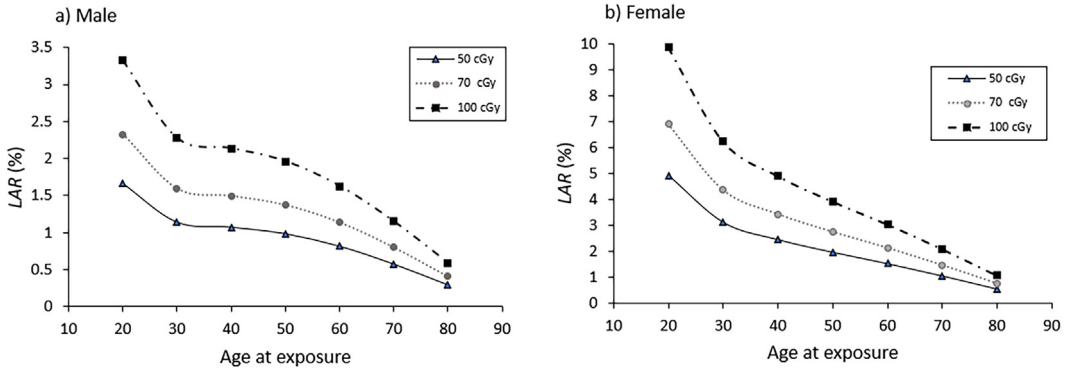

Fig. 2. Total LAR (in %) for the three prescription doses as a function of age for male (a) and female (b). Lines were added for better visualization of data.

perfusion study, when the prescription dose of radiotherapy treatment is 50 cGy.

The articles referenced previously estimated effective doses and risk for individual scans. However, Sodickson et al [52] estimated effective doses and LAR for patients (mean age 57 years old) from all CT scans received throughout their life at a tertiary care academic medical center. From the 31,462 patients studied, 15% received estimated cumulative effective doses of more than 100 mSv, and 4% received between 250 and 1375 mSv, which are of the same order of magnitude or higher than COVID-19 LDRT effective doses calculated in this study. In the same work, they obtained mean and maximum LAR values of 0.3% and 12% for cancer incidence. Our results are within this range. For example, 7% of the cohort had estimated LAR greater than 1%, which is the value obtained for LAR in this work for a 50 years old male and half of that obtained for a 50 year-old female (for the 50 cGy prescription dose).

Regarding risk to site-specific cancers, for a parathyroid 4DCT, Hoang et al. [48] obtained a value of LAR of lung cancer incidence of 0.068% and 0.134% for a 25 year-old male and female, respectively. These LAR estimates are consistently 11 and 13 times lower than the values found in our work for a 20 year-old male and female, respectively (for the 50 cGy prescription dose). Hosseini Nasab et al. [50] estimated, in cardiac CT angiography, LAR of lung cancer incidence of 0.04% and 0.11% for a 20 year-old male and female respectively. Additionally, Wook Kim et al. [53] estimated, for a total of 30 scans of kV CBCT, performed to position a patient during radiation for pelvic tumours, a LAR of cancer incidence that can reach a value of 4% for major organs (e.g., 4 % for colon and 2.8% for bladder in female of mixed ages). This value is higher than the maximum result obtained for organs LAR in this study, for a prescription dose of 50 cGy (2.1% of breast cancer incidence for 20 year-old female).

In the literature, the difficulties of some radiotherapy calculation algorithms managing areas of high tissue heterogeneity, such us lungs, have been described [54]. The calculation model used in this article is a Collapsed Cone Convolution Superposition algorithm (CCCS). It is known that the gold standard in radiotherapy calculations is Monte Carlo. However, for large field sizes and 6 MV, discrepancies in dose calculations should not be higher than 3–4% for CCCS algorithms [54].

An additional contribution of radiation dose to the patient comes from image-guided radiation therapy (IGRT). Depending on the technique used, the magnitude of this added dose is

Table 3
Effective doses from different radiology techniques and LDRT for COVID-19. *Depending on imaging device and low dose or standard dose mode. **180 mSv for transjugular intrahepatic portosystemic shunt placement and 166 mSv (61.2–380.8 mSv) for abdominal aortic endoprosthesis. CBCT: Cone Beam CT. kV: kilovoltage. MV: Megavoltage. CT: Computed Tomography. PET: Positron Emission Tomography.

Modality	Technique	Protocol	Range of reported effective dose (mSv)	Study
Radiotherapy Positioning	kV CBCT	Head and neck	3.4–10.3*	Min Moon et al. [27]
		Thorax	1.1–23.7*	Kan et al. [28]
		Pelvis	4.1–22.7*	Halg et al. [29]
				Abuhaimed et al. [30]
				Yuasa et al. [31]
				Qiu et al. [32]
				Dzierma et al. [33]
	4D CBCT	Thorax	7.3–8.8	Yuasa et al. [31]
				Marchant and Joshi [34]
	MV CBCT	Pelvis/8 MU protocol	4.6–35.9	Halg et al. [29]
				Quinn et al.[35]
	Portal images MV	AP + lateral double exposure	16.4	Halg et al. [29]
		AP + lateral	4.4	
		AP	1.9	
Diagnostic	Fan beam CT	Head and Neck	0.9–4	Kan et al. [28]
		Thorax	4–18	Dzierma et al. [33]
		Abdomen	4–25	Halg et al. [29]
		4DCT	29.5	Mettler et al. [36]
				Shrimpton et al. [37]
	PET/CT	Various	13.45–32.2	Martí-Climen et al. [38]
				Kaushik et al. [39]
				Huang et al. [40]
				Quinn et al. [41]
	Myocardial perfusion study	Tc99-Sestamibi (1 day) stress/rest-Thalium201 chloride stress/rest	9–41	Mettler et al. [36]
	Cardiac CT	Various	2–28.3	Hausleiter et al.[42]
				Tavakoli et al. [43]
				Gerber et al. [44]
				Sabarudin et al. [45]
Treatment	Interventional	Various	5,4–180**	Falco et al. [46]
				Mettler et al. [36]
	Radiotherapy COVID-19 LDRT	AP/PA 6MV 50 cGy	204–213	This study
		AP/PA 6MV 70 cGy	286–298	
		AP/PA 6MV 100 cGy	408–426	

Table 4
LAR of cancer incidence (using BEIR VII methodology [35]) for different radiology techniques and LDRT for COVID-19.

Modality	Technique	Protocol	LAR (%)	Study
Diagnostic	Fan beam CT	Routine head	0.023 (20 years old female)	Smith-Bindman et al. [47] Hoang et al. [48]
		Routine chest	0.25 (20 years old female)	
		Multiphase abdomen and pelvis CT	0.4 (20 years old female)	
		Parathyroid 4DCT	0.19/0.4 (55/20 years old female)	
	PET/CT	Different protocols of whole body pet/ct scans	0.163–0.323 (male; 20 years old) 0.231–0.514 (female; 20 years old	Huang et al. [40]
	Myocardial perfusion study	Dual isotope (Thalium-201 + technetium-99 m) scan	0.2/0.25 (50 years old male/female)	Berrington de González et al. [49]
	Cardiac CT	Various	0.6 (20 years old female) 0.12/0.24 (for male /female; median age 56.84 years old	Smith-Bindman et al. [47] Hosseini Nasab et al. [50]
Treatment	Interventional	electrophysiological/device implantation procedures	Range 0.01–0.28 (mean age 68 years old)	Casella et al. [51]
	Radiotherapy	**AP/PA LINAC 6MV COVID-19 (Prescription of 50 cGy)**	**1.66/4.93 (20 years old man and woman) 0.81/1.52 (60 years old man/woman)**	**This study**

different. For a Truebeam thorax kV CBCT the additional dose would be less than 2% of the prescribed dose (when prescribing 100 cGy) at any point of the field of view [55–57]. However, higher values have also been reported for a thorax kV CBCT using other linacs and protocols [27–31]. MV CBCT or portal MV image can also result in higher doses [28]. When possible, it would be preferable to use kV radiographs to reduce dose to organs at risk. In case of using CBCT, low dose protocols should be chosen. When using high dose IGRT techniques, imaging dose could be substracted from prescription dose.

To our knowledge, there is no standard protocol to treat COVID-19 pneumonia and actual treatments are based on patients treated in the early part of the twentieth century, when x-ray technology was very different to that existing nowadays. Given the relevance of the closest organs to lungs (such as breast and heart), an approach focused on reducing the dose to these organs (and then, reducing the cancer risk) could imply the use of modern radiotherapy techniques, such as IMRT. A similar study for IMRT treatments, as the one presented in this work, could be carried out to evaluate if IMRT significantly improves the results in terms of projected total cancer risk. Furthermore, it has to be taken into account that the need to reduce risk is of particular importance for younger patients, especially females. At the moment, severe COVID-19 pneumonia is affecting mainly patients older than 60 years, those for whom cancer risk significantly reduces. If clinical trials confirm the suitability of LDRT for treating COVID-19 pneumonia and its use extends to younger patients, research in using IMRT techniques will be required.

In conclusion, the low prescription doses used in COVID-19 radiotherapy result in a very low dose to organs outside the treatment field and consequently, an extremely small risk of cancer induction (lower than 0.06 cases per 10000). However, there are several organs lying wholly or partially within the large fields employed, which contribute to increase the total risk (with doses between 1 and 10 mSv/cGy). Lung and breast, among the most radiosensitive organs, are within this highest dose region. In summary, non-negligible stochastic effects of cancer induction have been estimated for LDRT treatment (e.g., total LAR of 4% for a 50-year old woman treated with 100 cGy). We would like to draw the radiotherapy communitýs attention to the detriments associated with exposure, particularly women treated at a young age.

Disclosure of conflicts of interest

The authors have no relevant conflict of interest.

Acknowledgement

BSN acknowledges the support of FONDECYT REGULAR (N1181133).

Appendix A. Supplementary data

Supplementary data to this article can be found online at https://doi.org/10.1016/j.radonc.2020.09.051.

References

[1] McIntire F, JHHTSJ o M Smith, X-ray therapy in the treatment of pneumonia. 1937.33: 422–426.
[2] Scott WRJR, X-ray therapy in the treatment of acute pneumonia: report covering the use of X-ray therapy in the treatment of acute pneumonia at the Niagra Falls Memorial Hospital, from Oct. 1, 1937 to Sept. 30, 1938. 1939; 33: 331–349.
[3] Settle EB. The roentgen treatment of lobar pneumonia. Am J Roentgenol Radiat Ther 1941;45:591–9.
[4] Rousseau JP, Johnson WM, Harrell GT. The value of roentgen therapy in pneumonia which fails to respond to the sulfonamides. Radiology 1942;38:281–9.
[5] Rödel F, Keilholz L, Herrmann M, Sauer R, Hildebrandt G. Radiobiological mechanisms in inflammatory diseases of low-dose radiation therapy. Int J Radiat Biol 2007;83:357–66.
[6] Calabrese EJ, Dhawan G. How radiotherapy was historically used to treat pneumonia: could it be useful today?. Yale J Biol Med 2013;86:555–70.
[7] Venkatraman P, Joshua Sahay, Maidili T, Rajisha Rajan T, Poojac S. Breakthro of COVID-19 using radiotherapy treatment modalities. Radiother Oncol 2020;148:225–6. https://doi.org/10.1016/j.radonc.2020.04.024.
[8] Lara Pedro C, Burgos Javier, Macias David. Low dose lung radiotherapy for COVID-19 pneumonia. The rationale for a cost-effective anti-inflammatory treatment. Clin Transl Radiat Oncol 2020;23:27–9. https://doi.org/10.1016/j.ctro.2020.04.006.
[9] Kirkby Charles, Mackenzie Marc. Is low dose radiation therapy a potential treatment for COVID-19 pneumonia?. Radiother Oncol 2020;147:221. https://doi.org/10.1016/j.radonc.2020.04.004. S0167-8140(20)30185-7.
[10] ClinicalTrials.gov. National Library of Medicine (U.S.). COVID-19 Pneumonitis Low Dose Lung Radiotherapy (COLOR-19) (2020, may) Retrieved from https://clinicaltrials.gov/ct2/show/NCT04377477?cond=radiotherapy+covid&draw=2&rank=1.
[11] ClinicalTrials.gov. National Library of Medicine (U.S.). Low Dose Anti-inflammatory Radiotherapy for the Treatment of Pneumonia by COVID-19 (2020, may) Retrieved from https://clinicaltrials.gov/ct2/show/NCT04380818?cond=radiotherapy+covid&draw=2&rank=3.
[12] ClinicalTrials.gov. National Library of Medicine (U.S.). Radiation Eliminates Storming Cytokines and Unchecked Edema as a 1-Day Treatment for COVID-19 (RESCUE 1-19) (2020, april) Retrieved from https://clinicaltrials.gov/ct2/show/NCT04366791?cond=radiotherapy+covid&draw=2&rank=4.
[13] ClinicalTrials.gov. National Library of Medicine (U.S.). Low Dose Radiotherapy in COVID-19 (2020, May) Retrieved from https://clinicaltrials.gov/ct2/show/NCT04390412.
[14] Thomas Mulliez, Kurt Barbé, Mark de Ridder. Estimating lung cancer and cardiovascular mortality in female breast cancer patients receiving radiotherapy. Radiotherapy and Oncology. June 26, 2020.
[15] Monty Charles. Sources and effects of ionizing radiation: UNSCEAR Report 2000. J Radiol Protect 2001;21:83–5. https://doi.org/10.1088/0952-4746/21/1/609.
[16] ICRP. Adult reference computational phantoms. ICRP Publication 110. Ann ICRP 2009;39.
[17] Howell RM, Scarboro SB, Taddei PJ, Krishnan S, Kry SF, Newhauser WD. Methodology for determining doses to in-field, out-of-field and partially in-field organs for late effects studies in photon radiotherapy. Phys Med Biol. 2010;55:7009–23. 10.1 https://doi.org/088/0031-9155/55/23/S04.
[18] Sánchez-Nieto B, Medina-Ascanio KN, Rodríguez-Mongua JL, Doerner E, Espinoza I. Study of out-of-field dose in photon radiotherapy: A commercial treatment planning system versus measurements and Monte Carlo simulations. Med Phys 2020. https://doi.org/10.1002/mp.14356.
[19] International Commission on Radiological Protection. The 2007 Recommendations of the International Commission on Radiological Protection. ICRP Publication 103. Ann ICRP 2007;3:2–4.
[20] National Research Council (NRC). Health Risks from Exposure to Low Levels of Ionizing Radiation: BEIR VII Phase 2. Washington, DC: The National Academies Press; 2006.
[21] Shuryak I, Hahnfeldt P, Hlatky L, Sachs RK, Brenner DJ. A new view of radiation-induced cancer: integrating short- and long-term processes, Part II: Second cancer risk estimation. Radiat Environ Biophys 2009;48:275–86. https://doi.org/10.1007/s00411-009-0231-2.
[22] Schneider U. Mechanistic model of radiation-induced cancer after fractionated radiotherapy using the linear-quadratic formula. Med Phys 2009;36:1138–43. https://doi.org/10.1118/1.3089792.
[23] Schneider U, Zwahlen D, Ross D, Kaser-Hotz B. Estimation of radiation-induced cancer from three-dimensional dose distributions: concept of organ equivalent dose. Int J Radiat Oncol Biol Phys 2005;61:1510–5. https://doi.org/10.1016/j.ijrobp.2004.12.040.
[24] Schneider U, Sumila M, Robotka J. Site-specific dose-response relationships for cancer induction from the combined Japanese A-bomb and Hodgkin cohorts for doses relevant to radiotherapy. Theor Biol Med Model 2011;8:27. https://doi.org/10.1186/1742-4682-8-27.
[25] Fuji H, Schneider U, Ishida Y, et al. Assessment of organ dose reduction and secondary cancer risk associated with the use of proton beam therapy and intensity modulated radiation therapy in treatment of neuroblastomas. Radiat Oncol. 2013;8:255. Published 2013 Nov 1. https://doi.org/10.1186/1748-717X-8-255.
[26] Sánchez-Nieto B, Romero-Expósito M, Terrón JA, Sánchez-Doblado F. Uncomplicated and Cancer-Free Control Probability (UCFCP): A new integral approach to treatment plan optimization in photon radiation therapy. Phys Med 2017;42:277–84. https://doi.org/10.1016/j.ejmp.2017.03.025.
[27] Moon Young Min, Kim Hyo-Jin, Kwak Dong Won, Kang Yeong-Rok, Lee Man Woo, Ro Tae-Ik, et al. Effective dose measurement for cone beam computed tomography using glass dosimeter. Nucl Eng Technol 2014;46:255–62.
[28] Kan MW, Leung LH, Wong W, Lam N. Radiation dose from cone beam computed tomography for image-guided radiation therapy. Int J Radiat Oncol Biol Phys 2008;70:272–9. https://doi.org/10.1016/j.ijrobp.2007.08.062.

[29] Halg RA, Besserer J, Schneider U. Systematic measurements of whole-body imaging dose distributions in image-guided radiation therapy. Med Phys 2012;39:7650–61. https://doi.org/10.1118/1.4758065.
[30] Abuhaimed A, Martin CJ, Sankaralingam M. A Monte Carlo study of organ and effective doses of cone beam computed tomography (CBCT) scans in radiotherapy. J Radiol Prot 2018;38:61–80. https://doi.org/10.1088/1361-6498/aa8f61.
[31] Yuasa Y, Shiinoki T, Onizuka R, Fujimoto K. Estimation of effective imaging dose and excess absolute risk of secondary cancer incidence for four-dimensional cone-beam computed tomography acquisition. J Appl Clin Med Phys 2019;20:57–68. https://doi.org/10.1002/acm2.12741.
[32] Qiu Yue, Moiseenko Vitali, Aquino-Parsons Christina. CherylEquivalent doses for gynecological patients undergoing IMRT or RapidArc with kilovoltage cone beam CT. Radiother Oncol 2012;104:257–62. https://doi.org/10.1016/j.radonc.2012.07.007.
[33] Dzierma Y, Minko P, Ziegenhain F, et al. Abdominal imaging dose in radiology and radiotherapy – Phantom point dose measurements, effective dose and secondary cancer risk. Phys Med 2017;43:49–56. https://doi.org/10.1016/j.ejmp.2017.10.019.
[34] Marchant TE, Joshi KD. Comprehensive Monte Carlo study of patient doses from cone-beam CT imaging in radiotherapy. J Radiol Protect 2017;37:13–30. https://doi.org/10.1088/1361-6498/37/1/13.
[35] Quinn A, Holloway L, Koh ES, et al. Radiation dose and contralateral breast cancer risk associated with megavoltage cone-beam computed tomographic image verification in breast radiation therapy. Pract Radiat Oncol 2013;3:93–100. https://doi.org/10.1016/j.prro.2012.05.003.
[36] Fred A. Mettler, Jr, Walter Huda, Terry T. Yoshizumi, Mahadevappa Mahesh. Effective doses in radiology and diagnostic nuclear medicine: A catalog. 2008. https://doi.org/10.1148/radiol.2481071451.
[37] Shrimpton PC, Jansen JT, Harrison JD. Updated estimates of typical effective doses for common CT examinations in the UK following the 2011 national review. Br J Radiol 2016;89:. https://doi.org/10.1259/bjr.20150346 20150346.
[38] Martí-Climent JM, Prieto E, Morán V, Sancho L, Rodríguez-Fraile M, Arbizu J, et al. Effective dose estimation for oncological and neurological PET/CT procedures. EJNMMI Res 2017;7:37. https://doi.org/10.1186/s13550-017-0272-5.
[39] Kaushik Aruna et al. Estimation of radiation dose to patients from (18) FDG whole body PET/CT investigations using dynamic PET scan protocol. Indian J Med Res 2015;142:721–31. https://doi.org/10.4103/0971-5916.174563.
[40] Huang Bingsheng, Law Martin Wai-Ming, Khong Pek-Lan. Whole-body PET/CT scanning: estimation of radiation dose and cancer risk. Radiology 2009;251(1):166–74.
[41] Quinn B, Dauer Z, Pandit-Taskar N, et al. Radiation dosimetry of 18F-FDG PET/CT: incorporating exam-specific parameters in dose estimates. BMC Med Imaging 2016;16:41. https://doi.org/10.1186/s12880-016-0143-y.
[42] Hausleiter J, Meyer T, Hermann F, et al. Estimated radiation dose associated with cardiac CT angiography. JAMA 2009;301:500–7. https://doi.org/10.1001/jama.2009.54.
[43] Tavakoli M, Faraji R, Alirezaei Z, Nateghian Z. Assessment of effective dose associated with coronary computed tomography angiography in Isfahan Province. Iran. J Med Signals Sens 2018;8:60–4.
[44] Gerber TC, Kantor B, McCollough CH (2009). Radiation dose and safety in cardiac computed tomography. Cardiol Clin, 27, 665–677. https://doi.org/1016/j.ccl.2009.06.006.
[45] Sabarudin A, Siong TW, Chin AW, et al. A comparison study of radiation effective dose in ECG-Gated Coronary CT Angiography and calcium scoring examinations performed with a dual-source CT scanner. Sci Rep 2019;9:4374. https://doi.org/10.1038/s41598-019-40758-5.
[46] Maria D Falco, Salvatore Masala, Matteo Stefanini , Paolo Bagalà , Daniele Morosetti, Eros Calabria et al, Effective-dose estimation in interventional radiological procedures, Radiol Phys Technol 2018;11:149–155. https://doi.org/10.1007/s12194-018-0446-5.
[47] Smith-Bindman R, Lipson J, Marcus R, et al. Radiation dose associated with common computed tomography examinations and the associated lifetime attributable risk of cancer. Arch Intern Med 2009;169:2078–86. https://doi.org/10.1001/archinternmed.2009.427.
[48] Hoang Jenny K, Reiman Robert E, Nguyen Giao B, Januzis Natalie, Chin Bennett B, Lowry Carolyn, et al. Lifetime attributable risk of cancer from radiation exposure during parathyroid imaging: comparison of 4D CT and parathyroid scintigraphy. Am J Roentgenol 2015;204:W579–85. https://doi.org/10.2214/AJR.14.13278.
[49] Berrington de Gonzalez A, Kim KP, Smith-Bindman R, McAreavey D. Myocardial perfusion scans: projected population cancer risks from current levels of use in the United States [published correction appears in Circulation. 2011 Jan 18;123(2):e10]. Circulation 2010;122:2403–10. https://doi.org/10.1161/CIRCULATIONAHA.110.941625.
[50] Nasab Seyed Mohammad Bagher Hosseini, Deevband Mohammad Reza, Shabestani-Monfared Ali, Amoli Seyed Ali Hoseini, Feyzabad Seyed Hasan Fatehi. Organ equivalent dose and lifetime attributable risk of cancer incidence and mortality associated with cardiac CT angiography. Radiat Prot Dosim 2020:1–11. https://doi.org/10.1093/rpd/ncaa033.
[51] Casella Michela, Dello Russo Antonio, Russo Eleonora, Catto Valentina, Pizzamiglio Francesca, Zucchetti Martina, et al. X-ray exposure in cardiac electrophysiology: A retrospective analysis in 8150 patients over 7 years of activity in a modern, large-volume laboratory. J Am Heart Assoc 2018;7:. https://doi.org/10.1161/JAHA.117.008233e008233.
[52] Sodickson A, Baeyens PF, Andriole KP, et al. Recurrent CT, cumulative radiation exposure, and associated radiation-induced cancer risks from CT of adults. Radiology 2009;251:175–84. https://doi.org/10.1148/radiol.2511081296.
[53] Dong Wook Kim, Weon Kuu Chung, Myonggeun Yoon, Imaging doses and secondary cancer risk from kilovoltage cone-beam ct in radiation therapy. Health Phys Soc (2013) https://doi.org/10.1097/HP.0b013e318285c685.
[54] Schwarz M, Cattaneo GM, Marrazzo L. Geometrical and dosimetrical uncertainties in hypofractionated radiotherapy of the lung: A review. Phys Med 2017;36:126–39. https://doi.org/10.1016/j.ejmp.2017.02.011.
[55] Ahmad Nobah, Saad Aldelaijan, Slobodan Devic, Nada Tomic, Jan Seuntjens, Mohammad Al-Shabanah et al. Radiochromic film based dosimetry of image-guidance procedures on different radiotherapy modalities. J Appl Clin Med Phys, 15, 2014.
[56] Giaddui Tawfik, Cui Yunfeng, Galvin James, Yan Yu, Xiao Ying. Comparative dose evaluations between XVI and OBI cone beam CT systems using Gafchromic XRQA2 film and nanoDot optical stimulated luminescence dosimeters. Med Phys 2013;40:. https://doi.org/10.1118/1.4803466062102.
[57] Chang Zheng, Qiuwen Wu, Adamson Justus, Ren Lei, Bowsher James, Yan Hui, et al. Commissioning and dosimetric characteristics of TrueBeam system: Composite data of three TrueBeam machines. Med Phys 2012;39:6981. https://doi.org/10.1118/1.4762682.